HTML ABSTRACT + LINKS

Free carrier absorption in Be-doped epitaxial AlGaAs thin films

M. B. M. Rinzan, D. G. Esaev, and A. G. U. Perera[a)]
Department of Physics and Astronomy, Georgia State University, Atlanta, Georgia 30303

S. G. Matsik
NDP Optronics LLC, 236 St. Martins Drive, Mableton, Georgia 30126

G. Von Winckel, A. Stintz, and S. Krishna
Center for High Technology Materials, ECE Department, University of New Mexico, Albuquerque, New Mexico 87106

(Received 12 April 2004; accepted 5 October 2004)

Free hole absorption in doped $Al_xGa_{1-x}As$ films, grown by molecular-beam epitaxy on semi-insulating GaAs substrates, was investigated. Free carrier absorption for three different hole concentrations with the same Al fraction and for two different Al fractions with the same doping concentration was studied. Experimental absorption coefficients were obtained from the data using a model that includes multiple reflections in the substrate wafer. In the 100–400 μm range, $(3,5,8)\times 10^{18}$ cm^{-3} Be-doped $Al_{0.01}Ga_{0.99}As$ films have absorption coefficients of $\sim(3,3.5,5)\times 10^{3}$ cm^{-1}, respectively, where the magnitude of the absorption is found to be almost independent of the wavelength. This allows replacing doped GaAs emitters in heterojunction interfacial work function internal photoemission far-infrared (HEIWIP) detectors with p-$Al_xGa_{1-x}As$ layers with $x<0.017$ facilitating the extension of the threshold wavelength of HEIWIP detectors beyond the 92 μm limit due to the practical Al fraction growth limit of 0.005 in molecular-beam epitaxy. © *2004 American Institute of Physics*. [DOI: 10.1063/1.1829383]

Recent developments in internal photoemission semiconductor junction infrared detectors[1–3] have made possible the realization of high performance homo- and heterojunction interfacial workfunction internal photoemission (HEIWIP) far-infrared (FIR) detectors operating up to $\sim$100 μm. The interest in the manipulation of these devices was stimulated in part by possible applications such as large focal plane arrays used for space astronomy as in NASA's Herschel program.[4] Present FIR detectors in use or under development for this wavelength range are extrinsic Ge photoconductors (stressed or unstressed),[5] and Ge (Ref. 6) and Si (Ref. 7) blocked-impurity-band (BIB) detectors. There are many technological challenges for fabricating Ge large format arrays, and GaAs BIB detectors are still in the developmental stages.

Although a threshold wavelength (λ_0) of 92 μm has been realized for p-GaAs/$Al_xGa_{1-x}As$ HEIWIPs, further extension is hindered by the practical growth limit of the aluminum fraction (0.005) in molecular-beam epitaxy (MBE)-grown $Al_xGa_{1-x}As$ barrier structures.[8] Even in HIWIPs, λ_0 was observed to be limited to $\sim$100 μm, as increasing the doping concentration above 2×10^{19} cm^{-3} would set off the depletion of free holes in the heavy hole band resulting in a shorter threshold wavelength.[9] Doped $Al_xGa_{1-x}As$ emitters and GaAs barriers avoid this limit allowing the realization of HEIWIP devices with the λ_0 extended beyond 138 μm.[8] In this mode, $Al_{0.01}Ga_{0.99}As$ emitters are expected to give a λ_0 of 325 μm. The operation mechanism of these detectors involves FIR absorption in doped $Al_xGa_{1-x}As$ emitters. This makes it important to understand the free carrier absorption in doped AlGaAs thin films, especially, in the FIR region where the extended wavelength detectors would operate. Experimental absorption coefficients for $Al_xGa_{1-x}As$ have been reported up to 20 μm, previously.[10] In this paper, results are reported on the free-hole absorption in Be-doped $Al_xGa_{1-x}As$ thin films in the wavelength range of 10–400 μm.

Four Be-doped $Al_xGa_{1-x}As$ thin films were grown by MBE on 520 μm thick semi-insulating GaAs(100) wafers. The samples were back side polished in order to reduce the reflection losses. The structure parameters, and the frequency and the wavelength of plasma resonance of free holes in the $Al_xGa_{1-x}As$ films are shown in Table I. Reflectance and transmittance measurements were performed for 3×10^{18}, 5×10^{18}, and 8×10^{18} cm^{-3} Be-doped $Al_{0.01}Ga_{0.99}As$ films and for two 5×10^{18} cm^{-3} Be-doped films with 0.01 and 0.20 Al fractions. One of the above samples was etched down using a wet etchant to obtain the transmittance and the reflectance spectra of the GaAs substrate. All measurements were performed at room temperature with a Perkin–Elmer system 2000 Fourier transform infrared spectrometer (FTIR) and a Si composite bolometer. For both the substrate sample and the film/substrate samples, transmittance was measured under a normal incidence geometry, while the reflectance was

TABLE I. Parameters of the measured $Al_xGa_{1-x}As$ thin-film samples. The 1 μm thick Be-doped $Al_xGa_{1-x}As$ films were grown on 520 μm thick semi-insulating GaAs substrates. Here, x is the Al fraction, p is the acceptor doping density, f_p and λ_p are the frequency and wavelength of the plasma resonance of free carriers in the films, respectively.

Sample	Al x	p ($\times 10^{18}$ cm^{-3})	f_P (THz)	λ_P (μm)
1442	0.01	3	6.6	45.2
1443	0.01	5	8.6	35.0
1444	0.01	8	10.9	27.6
1446	0.20	5	8.3	36.3

[a)]Also at: NDP Optronics LLC; electronic mail: uperera@gsu.edu

 © 2004 American Institute of Physics
Downloaded 09 Dec 2004 to 131.96.4.66. Redistribution subject to AIP license or copyright, see http://apl.aip.org/apl/copyright.jsp

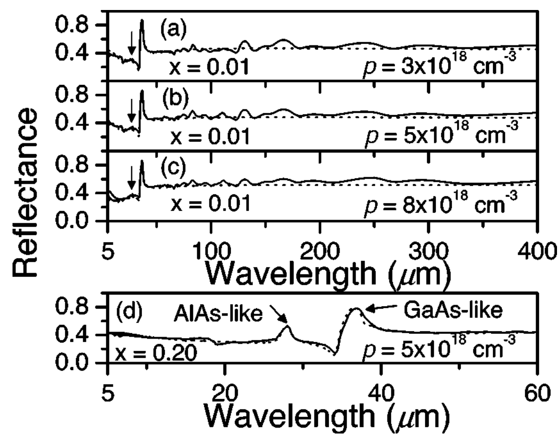

FIG. 1. Experimental (solid line) and model (dashed line) reflectance spectra for 1 μm thick Be-doped $Al_{0.01}Ga_{0.99}As$ epitaxial films grown on 520 μm thick GaAs semi-insulating substrates for different doping concentrations: (a) 3×10^{18}, (b) 5×10^{18}, and (c) 8×10^{18} cm^{-3}. The sharp peaks at $\sim$37 μm are due to the interaction of radiation with GaAs-like TO phonons, while the arrows at $\sim$28 μm point to small peaks due to interaction with AlAs-like TO phonons. The ripples toward the FIR end are due to the Fabry–Pérot interference in the semi-insulating substrate. (d) Experimental and model reflectance spectra for 1 μm thick 5×10^{18} cm^{-3} Be-doped $Al_{0.20}Ga_{0.80}As$ epitaxial film on a similar substrate.

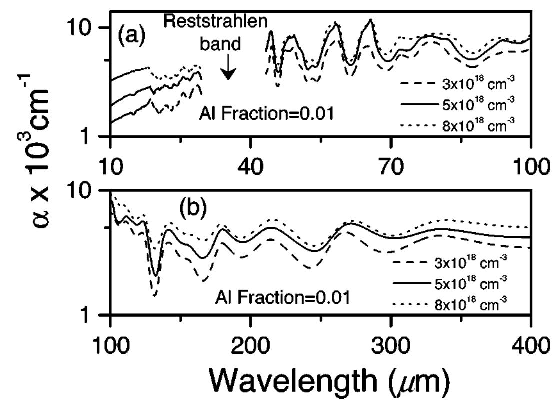

FIG. 2. (a) Experimental free-hole absorption coefficient (α) in the range of 10–100 μm for Be-doped $Al_{0.01}Ga_{0.99}As$ thin films at room temperature. The dashed, solid, and dotted curves show α for 3, 5, and 8×10^{18} cm^{-3}, respectively. The region shown by the break corresponds to the reststrahlen region of $Al_{0.01}Ga_{0.99}As$. (b) The α is almost independent of wavelength in the FIR range of 100–400 μm, and $\sim(3,3.5,\text{and }5)\times10^3$ cm^{-1} for $(3,5,\text{and }8)\times10^{18}$ cm^{-3} Be-doped $Al_{0.01}Ga_{0.99}As$ epitaxial films, respectively.

measured at near normal incidence, $\sim5°$, using the specular reflectance accessory. The FTIR resolution was 4 cm^{-1}.

The complex permittivity $\varepsilon(\omega)$ for the doped $Al_xGa_{1-x}As$ films was modeled using the Drude theory[11] for free carriers in combination with an additive two oscillator mode for phonons:[10]

$$\varepsilon(\omega)=\varepsilon_\infty\left[1-\frac{\omega_p^2}{\omega(\omega+i\omega_0)}\right]+\sum_j\frac{S_j\omega_{\mathrm{TO}_j}^2}{\omega_{\mathrm{TO}_j}^2-\omega^2-i\omega\gamma_j}. \quad (1)$$

The first term in Eq. (1) describes the interaction of infrared radiation with the free carriers in the doped $Al_xGa_{1-x}As$ film. Here, ε_∞ is the high-frequency dielectric constant, ω is the frequency of incident radiation, $\omega_0=1/\tau$ is a free carrier damping constant with a relaxation time of τ, $\omega_p=\sqrt{pq^2/\varepsilon_\infty\varepsilon_0 m^*}$ is the plasma frequency of free carriers with effective mass m^* and concentration p, and q is the magnitude of the electron charge. The second term describes the interaction of radiation with GaAs-like and AlAs-like transverse optical (TO) phonons in the frame of Lorentz model. Here, ω_{TO_j} is the TO-phonon frequency, γ_j is a damping constant for TO phonons, and S_j is the TO-phonon oscillator strength. A single oscillator with GaAs TO phonons was used for the GaAs substrate.

The model reflectance spectra of the $Al_xGa_{1-x}As$ films on the GaAs substrates, and the substrate alone were calculated using the complex permittivities $\varepsilon(\omega)$ of the films and the substrate with a free carrier relaxation time of $\tau=1.2\times10^{-14}$ s.[12] The dielectric constants and the TO-phonon parameters for the films and the optical constants used for the GaAs bulk substrate were from Ref. 10. The model absorption coefficient, α, of the film was calculated using $\alpha=2(\omega/c)\hat{k}(\omega)$, where $\hat{k}(\omega)$ is the extinction coefficient equal to the imaginary part of $\sqrt{\varepsilon(\omega)}$ and c is the speed of light.

The model reflectance spectra based on Eq. (1) and the experimental spectra for the $Al_{0.01}Ga_{0.99}As$ films on GaAs substrates at room temperature are shown in Figs. 1(a)–1(c). The sharp peak in the spectra at $\sim$37 μm is due to the interaction of radiation with GaAs-like TO phonons, while the arrows at $\sim$28 μm point to a small peak caused by the interaction of AlAs-like TO phonons. Except for these two phonon peaks, the difference in the reflectance between a single-oscillator and a double-oscillator model is negligible for $x<0.20$. The model and experimental reflectance for $Al_{0.20}Ga_{0.80}As/GaAs$ sample around the reststrahlen band are shown in Fig. 1(d). Here, it is clear that the increased Al fraction, $x=0.20$, has increased the strength of the AlAs-like phonon while decreasing the GaAs-like phonon strength. Reflectance spectra for all samples showed an intensity oscillation in the FIR range. Reflectance measurements with 1 cm^{-1} FTIR resolution showed an oscillation periodicity of 2.7 ± 0.1 cm^{-1}, which corresponds to the Fabry–Pérot interference caused by the 520 μm thick substrate. Therefore, the experimental absorption coefficient of the films was calculated using a model [Eqs. (2) and (3)] that includes the multiple reflections within the GaAs substrate. The multiple reflections inside the film layer were not included due to the low reflectivity, $\sim$0.03, of the $Al_xGa_{1-x}As/GaAs$ interface

$$\alpha_{\mathrm{Film}}d_{\mathrm{Film}}+\alpha_{\mathrm{Sub}}d_{\mathrm{Sub}}=\sinh^{-1}\left[\frac{(1-R_{\mathrm{sample}})^2-T_{\mathrm{sample}}^2}{2T_{\mathrm{sample}}}\right], \quad (2)$$

$$\alpha_{\mathrm{Sub}}d_{\mathrm{Sub}}=\sinh^{-1}\left[\frac{(1-R_{\mathrm{Sub}})^2-T_{\mathrm{Sub}}^2}{2T_{\mathrm{Sub}}}\right]. \quad (3)$$

The experimental free-hole absorption coefficient spectra for the three $Al_{0.01}Ga_{0.99}As$ films with different Be doping densities are shown in Figs. 2(a) and 2(b). The dashed curve shows α for 3×10^{18} cm^{-3}, while the solid and the dotted curves are for 5×10^{18} and 8×10^{18} cm^{-3}, respectively. The absorption coefficients, α, were obtained for room temperature using the experimental transmittance and reflectance data in Eqs. (2) and (3), except for the reststrahlen region. The experimental transmittance in that region (falling well inside the spectrometer noise level due to the high reflectance of both the GaAs substrate layer and the $Al_xGa_{1-x}As/GaAs$ samples in the reststrahlen region) will blow up Eqs. (2) and (3) making it impossible to calculate α.

Downloaded 09 Dec 2004 to 131.96.4.66. Redistribution subject to AIP license or copyright, see http://apl.aip.org/apl/copyright.jsp

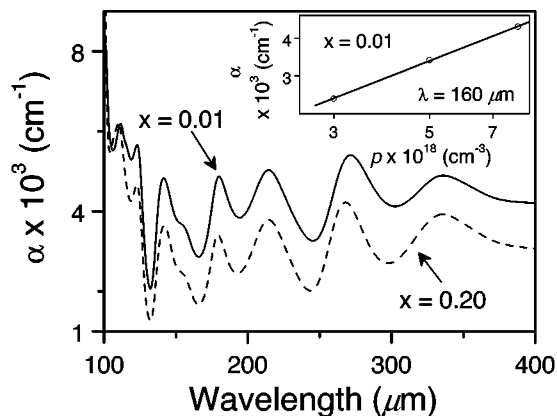

FIG. 3. Experimental free-hole absorption coefficient (α) at room temperature for Be-doped $Al_xGa_{1-x}As$ thin films in the FIR range of 100–400 μm. The solid and the dashed curves show α for $x=0.01$ and $x=0.20$ films, respectively. The free-hole absorption is found to be almost independent of wavelength in the 100–400 μm range. The α has decreased from $\sim 3.5 \times 10^3$ at $x=0.01$ to $\sim 3\times 10^3$ cm^{-1} at $x=0.20$. The inset shows a sublinear relationship of the free-hole absorption coefficient with a Be-doping density, $\alpha \propto p^{0.5}$, for $Al_{0.01}Ga_{0.99}As$ films at 160 μm.

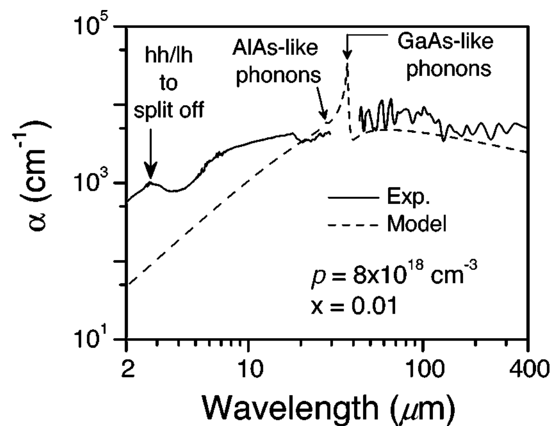

FIG. 4. The model and experimental free-hole absorption coefficient for a 8×10^{18} cm^{-3} Be-doped $Al_{0.01}Ga_{0.99}As$ film from 2 to 400 μm at room temperature. The peak around 3 μm is due to carrier transitions from the heavy hole (hh) and light hole (lh) bands to the split off band of $Al_{0.01}Ga_{0.99}As$.

No major changes in α are expected with temperature due to minute temperature coefficients associated with the relevant optical constants for $Al_xGa_{1-x}As$.[10] Figure 2(b) shows α increasing from around 3×10^3 to 5×10^3 cm^{-1} as doping density increases from 3×10^{18} to 8×10^{18} cm^{-3}. Although a $\sim\lambda^2$ dependency is observed in the shorter-wavelength region, the free-hole absorption is found to be almost independent of the wavelength in the range of 100–400 μm.

Free-hole absorption coefficient spectra for films with two different x values with the same doping density, 5×10^{18} cm^{-3}, are shown in Fig. 3. The α has decreased from $\sim 3.5\times 10^3$ at $x=0.01$ to 3×10^3 cm^{-1} at $x=0.20$, while being wavelength independent in the range of 100–400 μm. The GaAs emitter/$Al_xGa_{1-x}As$ barrier HEIWIP devices can only have a maximum λ_0 of 92 μm due to the practical Al fraction growth limit of ~ 0.005 in MBE. However, in devices with doped $Al_xGa_{1-x}As$ emitters, λ_0 increases with x, avoiding the growth limitation. Using a detector with doped $Al_{0.01}Ga_{0.99}As$ layers as emitters, a λ_0 of ~ 325 μm could be obtained for a structure with intrinsic GaAs barriers. Further, calculations show that the FIR absorption coefficient in the range of 5–400 μm decreases by $\sim 0.5\%$ only, when a 5×10^{18} cm^{-3} Be-doped GaAs emitter is replaced with an $Al_{0.01}Ga_{0.99}As$ emitter of similar doping. Hence, FIR absorption, almost similar to GaAs can be obtained using emitter layers with lower Al fractions. The inset of Fig. 3 shows a sublinear relationship between α and the acceptor doping density (p) at 160 μm for $x=0.01$ films. The α is proportional to $\sim p^{0.5}$. Therefore, the FIR absorption in the $Al_xGa_{1-x}As$ film layers increases with the doping density.

The calculated and the experimental absorption coefficient spectra for the $Al_{0.01}Ga_{0.99}As$ film with 8×10^{18} cm^{-3} doping concentration are shown in Fig. 4. The peak in the experimental curve around 3 μm is due to the photoexcitation from heavy and light hole bands to the split off band of $Al_xGa_{1-x}As$, which is not included in the model spectrum.

In conclusion, free carrier absorption in the range of 10–400 μm has been investigated. The absorption coefficient for $Al_{0.01}Ga_{0.99}As$ is almost the same for GaAs, and this facilitates the use of thin acceptor-doped $Al_xGa_{1-x}As$ absorber layers as emitters in threshold extension of HEIWIP FIR detectors. The sublinear relationship between the absorption coefficient and the doping density would be useful in designing HEIWIP detectors. Since the variation of α with the Al fraction is not significant for small Al fractions, the absorption quantum efficiency for HEIWIPs with different threshold wavelengths will not vary significantly.

This work was supported in part by NASA under NNC 04CA85C, and the NSF under Grant No. ECS-0140434. One of the authors (M.B.M.R.) is supported by GSU RPE funds. The authors acknowledge fruitful discussions with Dr. H. C. Liu at the National Research Council, Canada.

[1] P. W. Pellegrini and J. R. Jimenez, *The Physics of Thin Films* (Academic, New York, 1998), Vols. 24 and 115.
[2] T. L. Lin, J. S. Park, S. D. Gunapala, E. W. Jones, and H. M. Del Castillo, Opt. Eng. (Bellingham) **33**, 716 (1994).
[3] D. G. Esaev, S. G. Matsik, M. B. M. Rinzan, A. G. U. Perera, H. C. Liu, and M. Buchanan, J. Appl. Phys. **93**, 1879 (2003).
[4] G. L. Pilbratt, *The Promise of the Herschel Space Observatory* (ESA, Netherlands, 2001), pp. 13–20.
[5] E. E. Haller, Infrared Phys. Technol. **35**, 127 (1994).
[6] D. M. Watson, M. T. Guptill, J. E. Huffman, T. N. Krabach, S. N. Raines, and S. Satyapal, J. Appl. Phys. **74**, 4199 (1993).
[7] J. E. Huffman, A. G. Crouse, B. L. Halleck, T. V. Downes, and T. L. Herter, J. Appl. Phys. **72**, 273 (1992).
[8] S. G. Matsik, M. B. M. Rinzan, A. G. U. Perera, H. C. Liu, Z. R. Wasilewski, and M. Buchanan, Appl. Phys. Lett. **82**, 139 (2003).
[9] A. G. U. Perera, S. G. Matsik, M. B. M. Rinzan, A. Weerasekara, M. Alevli, H. C. Liu, M. Buchanan, B. Zvonkov, and V. Gavrilenko, Infrared Phys. Technol. **44**, 347 (2003).
[10] S. Adachi, *GaAs and Related Materials* (World Scientific, Singapore, 1994).
[11] J. S. Blakemore, J. Appl. Phys. **53**, R123 (1982).
[12] M. L. Huberman, A. Ksendzov, A. Larsson, R. Terhune, and J. Maserjian, Phys. Rev. B **44**, 1128 (1991).

Downloaded 09 Dec 2004 to 131.96.4.66. Redistribution subject to AIP license or copyright, see http://apl.aip.org/apl/copyright.jsp